

## THE METHOD OF WEIGHTED RESIDUALS FOR TRANSVERSELY ISOTROPIC AXISYMMETRIC PROBLEMS AND ITS APPLICATIONS TO ENGINEERING

Zhang Liangchi and Ding Haojiang  
(Zhejiang University)

**ABSTRACT:** A method with two harmonic functions is proposed for solving transversely isotropic axisymmetric problems by applying the theorems of Refs. [1] and [5]. A series of simple formulas of the boundary least square collocation method is derived. Two engineering examples show that the present method is much more convenient than Lekhniskii's with biharmonic functions. Some useful conclusions are finally obtained.

**KEY WORDS:** the method of weighted residuals (MWR), transverse isotropy, axisymmetric problems, harmonic function.

### I. INTRODUCTION

The analyses of transversely isotropic axisymmetric problems in engineering have been the subject of many experts<sup>[2-5]</sup>. As early as the 1950s, Hu Haichang and Lekhniskii solved some typical problems with biharmonic functions<sup>[4]</sup>.

In the present paper, a method with two harmonic functions is proposed for solving axisymmetric problems by applying the theorems of Refs. [1] and [5]. This method is convenient to find analytical solutions because thorough analyses of harmonic functions have been made. Moreover, it is also very suitable for the applications of MWR since a series of simple formulas can be derived. The paper analyzes two engineering examples with the boundary least square collocation method and gets very good results and advances some opinions on the point-load tests.

### II. DERIVATION OF EQUATIONS

It is convenient to use the cylindrical coordinates  $(r, z)$  for the analyses of transversely isotropic axisymmetric elastic bodies. The general solutions of the title problem can be easily obtained from the theory of Ref. [2]:

$$u_r = \sum_{j=1}^2 \left( -\frac{\partial \varphi_j}{\partial r} \right) \quad u_z = - \sum_{j=1}^2 \left( \frac{\alpha - \gamma s_j^2}{s_j^2} \right) \frac{\partial \varphi_j}{\partial z} \quad (1)$$

$$\left( \frac{\partial^2}{\partial r^2} + \frac{1}{r} \frac{\partial}{\partial r} + \frac{1}{s_j^2} \frac{\partial^2}{\partial z^2} \right) \varphi_j = 0 \quad (j = 1, 2) \quad (2)$$

where

$$s_{1,2} = \left[ \gamma^2 + \alpha\beta - 1 \pm \sqrt{(\gamma^2 + \alpha\beta - 1)^2 - 4\alpha\beta\gamma^2} \right] / (2\beta\gamma)$$

$$\alpha = B_{11}/B_{13} \quad \beta = B_{33}/B_{13} \quad \gamma = B_{44}/B_{13} \quad (3)$$

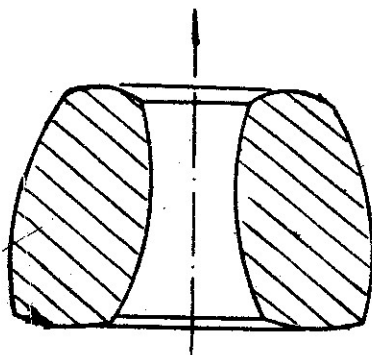


Fig.1 A multiply connected region

The corresponding expressions of stresses can then be derived from equation (1). For a simply connected region, Equ.(2) has solutions of form

$$\varphi_j(r,s,z) = \sum_{n=1}^{\infty} \omega_n^j \phi_n(r,s,z) \quad (j = 1,2) \quad (4)$$

but for a multiply connected region as shown in Fig.1, the following additional functions should be superposed

$$\bar{\varphi}_j(r,s,z) = \sum_{n=1}^{\infty} \lambda_n^j [ \phi_n(r,s,z) \ln r + Q_n(r,s,z) ], \quad (j = 1,2) \quad (5)$$

where  $\omega_n^j$  and  $\lambda_n^j$  are undetermined coefficients, and  $Q_n$  and  $\phi_n$  are homogeneous and homogeneous harmonic polynomials of the  $n$ th order, respectively. For the sake of convenience and definiteness, the following notations are adopted:

$$\phi_n = \phi_n(r,z), \quad \phi_n^j = \phi_n(r,s,z), \quad Q_n = Q_n(r,z), \quad Q_n^j = Q_n(r,s,z).$$

The following recurrence formulas are used

$$\left\{ \begin{array}{l} \phi_n = z\phi_{n-1} - \frac{r^2}{n} \psi_{n-1}, \quad \phi_0 = 1 \\ \psi_n = n\phi_{n-1} + z\psi_{n-1}, \quad \psi_0 = 0 \\ Q_n = zQ_{n-1} - \frac{r^2}{n} \pi_{n-1}, \quad Q_0 = 0 \\ \pi_n = nQ_{n-1} + z\pi_{n-1} - \frac{2}{n+1} \psi_n, \quad \pi_0 = 0 \end{array} \right. \quad (6)$$

and

(3)

$$\begin{cases} \frac{\partial \phi_n}{\partial r} = -r\psi_{n-1} & \frac{\partial \phi_n}{\partial z} = n\phi_{n-1} & \frac{\partial^2 \phi_n}{\partial r \partial z} = -nr\psi_{n-2} \\ \frac{\partial^2 \phi_n}{\partial r^2} = \psi_{n-1} - n(n-1)\phi_{n-2} & \frac{\partial^2 \phi_n}{\partial z^2} = n(n-1)\phi_{n-2} \\ \frac{\partial Q_n}{\partial r} = -r\pi_{n-1} & \frac{\partial Q_n}{\partial z} = nQ_{n-1} & \frac{\partial^2 Q_n}{\partial r \partial z} = -nr\pi_{n-2} \\ \frac{\partial^2 Q_n}{\partial r^2} = \pi_{n-1} + 2\psi_{n-1} - n(n-1)Q_{n-2} \\ \frac{\partial^2 Q_n}{\partial z^2} = n(n-1)Q_{n-2} \end{cases} \quad (7)$$

With the help of Eqs.(6) and (7), the components of stresses and displacements can be expressed as

$$\begin{pmatrix} u_r \\ u_z \\ \sigma_\theta \\ \sigma_z \\ \tau_{rz} \end{pmatrix} = \sum_{n=1}^{\infty} \sum_{j=1}^2 \left( \omega_n^j \begin{pmatrix} u_{nj}^r \\ u_{nj}^z \\ B_{66} \sigma_{nj}^\theta \\ B_{66} \sigma_{nj}^z \\ B_{66} \sigma_{nj}^{rz} \end{pmatrix} + \lambda_n^j \begin{pmatrix} \bar{u}_{nj}^r \\ \bar{u}_{nj}^z \\ B_{66} \bar{\sigma}_{nj}^\theta \\ B_{66} \bar{\sigma}_{nj}^z \\ B_{66} \bar{\sigma}_{nj}^{rz} \end{pmatrix} \right) \quad (8)$$

where  $u_{nj}^r, \bar{u}_{nj}^r$  and so on are the functions of  $\phi_n^j, \psi_n^j, Q_n^j$ , and  $\pi_n^j$ . The approximate representations of stresses and displacements are obtained by truncating Equ.(8) and can be determined once the coefficients  $\omega_n^j$  and  $\lambda_n^j$  are solved from the linear equations of residuals

$$\int_{\partial\Omega} \underline{W}_{\partial\Omega} \underline{R}_{\partial\Omega} ds = \underline{0},$$

where  $\underline{R}_{\partial\Omega}$  is the vector of boundary residuals and can be calculated with the aid of proper boundary conditions of region  $\Omega$ , and  $\underline{W}_{\partial\Omega}$  is a weight matrix<sup>[6]</sup>.

### III. THE CALCULATIONS AND ANALYSES OF ENGINEERING EXAMPLES

Many significant problems have been analyzed by the above formulas, but only two of them will be given in this paper to illustrate the characters and advantages of the present method. The boundary least square collocation method is employed and the relation

$$G_{\perp} = \frac{E_{\perp}}{2(1 + \nu_{\perp})}$$

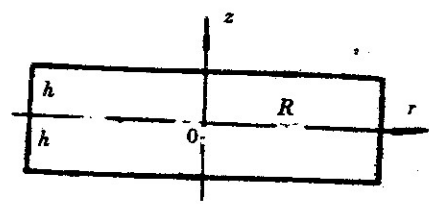


Fig.2 A magnesium cylinder

is used throughout the calculations.

**Example 1.** A magnesium finite cylinder with transverse isotropy is subjected to a self-equilibrium end stresses prescribed as

$$z = \pm h: \quad \sigma_z = 1 - 2r^2 \quad \tau_{rz} = 0$$

The elastic coefficients of the material are taken from Ref. [3]. The end problems of the circular cylinders have been the focus of much research attention over many decades and have widely been investigated<sup>[3,7]</sup>. Generally, the methods of eigenfunctions or Fourier series are employed. In order to obtain results with good accuracy, a large number of terms of the corresponding series should usually be taken, because of the slow convergence. In 1978, Vendhan and Archer calculated magnesium cylinders with fifty-three terms of the eigenfunction expansion<sup>[3]</sup>. In this paper, we take twenty-two and twenty terms of Eq.(8) for the cylinders of  $h/R = 0.05$  and  $h/R = 0.2$ , respectively. The results of  $\sigma_r$  and  $\sigma_\theta$  on section  $z = 0$  are listed in Table 1.

Table 1  
Stresses on the section  $z = 0$  of the magnesium cylinder

$r/R$	0.0	0.1	0.2	0.3	0.4	0.5	0.6	0.7	0.8	0.9	1.0
$\sigma_r$											
$h/R = 0.05$	0.0988	0.0978	0.0947	0.0897	0.0826	0.0735	0.0623	0.0492	0.0340	0.0169	0.0000
$h/R = 0.20$	0.0666	0.0657	0.0627	0.0576	0.0505	0.0417	0.0316	0.0214	0.0135	0.0063	0.0000
$\sigma_\theta$											
$h/R = 0.05$	0.0988	0.0957	0.0866	0.0715	0.0502	0.0229	-0.0105	-0.0500	-0.0955	-0.1491	-0.2033
$h/R = 0.20$	0.0666	0.0636	0.0545	0.0393	0.0181	-0.0092	-0.0424	-0.0810	-0.1238	-0.1669	-0.2100

The comparison of  $\sigma_\theta$  (for  $h/r = 0.05$ ) from Table 1 with the Vendhan's results has been shown in Fig.3. The curves show that the present results are in good agreement with Vendhan's, but the present method is more labour-saving and more forthright on the procedure of calculation.

**Example 2.** The axisymmetric ellipsoidal point-load rock specimen, as shown in Fig.4, is a typical one in the point-load tests, which are used to determine the strength of rock which has lower strength or has severely been weathered so that normal tests become powerless. Unfortunately, up to now, either in theoretical studies or in experimental investigations the rock specimen has been considered as isotropic<sup>[8]</sup>. In order to simulate the properties of the materials more exactly, we adopt the model of transverse isotropy for the first time. The elastic coefficients are taken as:  $E_{\perp} = 1.0 \times 10^5 \text{ kg/cm}^2$ ,  $\nu_{\perp} = 0.3$  and  $\nu_{11} = 0.25$ , and three different values of  $E_{11}$

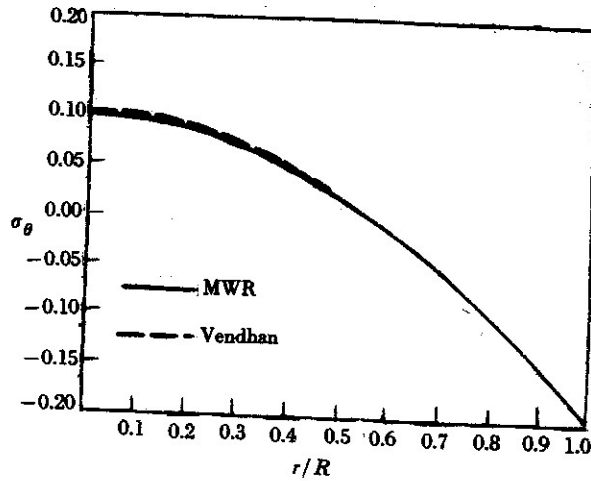


Fig.3 Comparison of  $\sigma_\theta$  on section  $z = 0$

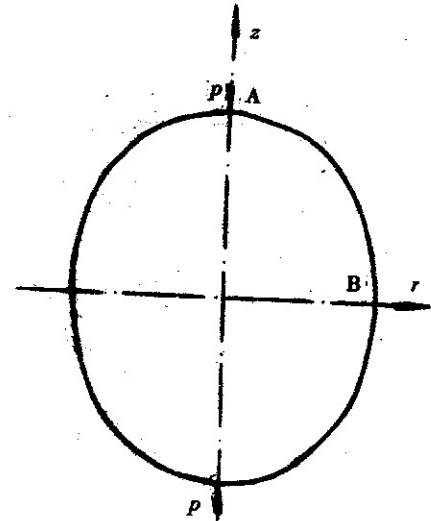


Fig.4 An ellipsoidal rock specimen for point-load test

are taken: a)  $E_{11} = 1.40 \times 10^5 \text{kg/cm}^2$ ; b)  $E_{11} = 1.45 \times 10^5 \text{kg/cm}^2$  and c)  $E_{11} = 1.50 \times 10^5 \text{kg/cm}^2$  in order to investigate the variation of stresses of the specimen with different elastic coefficients. The dimensions of the specimen are  $OA = 2.63 \text{cm}$  and  $OB = 2.0\text{cm}$ . Here we take eighteen terms of Equ.(8) as the trial function. Tables 2 and 3 list the stresses of the above three cases.

Table 2  
Stresses ( $\text{kg/cm}^2$ ) on the loading axis of the ellipsoidal specimen

$z(\text{cm})$	$E_{11}$			$\sigma_r$			$\sigma_z$		
	a	b	c	a	b	c	a	b	c
0.0	0.6836	0.6646	0.6457	-3.3115	-3.3105	-3.3104			
0.2	0.6889	0.6700	0.6511	-3.3820	-3.3808	-3.3805			
0.4	0.7027	0.6835	0.6642	-3.5987	-3.5968	-3.5960			
0.6	0.7195	0.6993	0.6791	-3.9808	-3.9779	-3.9760			
0.8	0.7326	0.7106	0.6885	-4.5693	-4.5648	-4.5616			
1.0	0.7339	0.7084	0.6827	-5.4407	-5.4341	-5.4291			
1.2	0.7181	0.6854	0.6524	-6.7411	-6.7307	-6.7223			
1.4	0.7000	0.6549	0.6122	-8.7597	-8.7424	-8.7279			
1.6	0.6630	0.5996	0.5353	-12.0715	-12.0430	-12.0185			
1.8	0.5777	0.4842	0.3899	-17.8600	-17.8090	-17.7640			
2.0	0.1534	0.0046	-0.1458	-28.7373	-28.6279	-28.5288			

Table 3

Stresses (kg/cm<sup>2</sup>) on the section  $z = 0$  of the ellipsoidal specimen

$r(\text{cm})$	$\sigma_r$			$\sigma_\theta$			$\sigma_z$		
	a	b	c	a	b	c	a	b	c
0.0	0.6836	0.6646	0.6457	0.6836	0.6646	0.6457	-3.3115	-3.3105	-3.3104
0.2	0.6619	0.6432	0.6247	0.6876	0.6694	0.6514	-3.2505	-3.2492	-3.2489
0.4	0.5999	0.5822	0.5646	0.6985	0.6826	0.6668	-3.0752	-3.0733	-3.0723
0.6	0.5059	0.4897	0.4736	0.7132	0.7007	0.6883	-3.8068	-2.8043	-2.8026
0.8	0.3896	0.3752	0.3609	0.7275	0.7188	0.7104	-2.4741	-2.4713	-2.4691
1.0	0.2579	0.2453	0.2326	0.7359	0.7312	0.7267	-2.1068	-2.1042	-2.1021
1.2	0.1078	0.0964	0.0850	0.7314	0.7302	0.7292	-1.7306	-1.7292	-1.7278
1.4	-0.0191	-0.0297	-0.0386	0.7010	0.7024	0.7041	-1.3671	-1.3675	-1.3677
1.6	-0.0622	-0.0708	-0.0731	0.6073	0.6103	0.6136	-1.0705	-1.0740	-1.0771
1.8	-0.0293	-0.0315	-0.0324	0.5400	0.5457	0.5537	-0.9479	-0.9566	-0.9695
2.0	0.0000	0.0000	0.0000	0.4757	0.4869	0.4983	-0.8671	-0.8893	-0.9017

## IV. CONCLUSIONS

The following conclusions can be obtained from above analyses and discussions:

1. By the use of Eqs.(7) and (8), we can make the boundary least square collocation method for solving the transversely isotropic axisymmetric problems as simple as the corresponding isotropic ones. The present method is much more forthright than Lekhnitskii's with biharmonic functions.
2. The present method can provide approximate analytical solutions. It is therefore more convenient for determining the locations of the characteristic points of stresses, such as extreme value points, zero points and so on. These special points are very useful for understanding the stress distributions in the specimen.
3. This paper considers for the first time the point-load rock specimen as a transversely isotropic one, thus several valuable results which cannot be gotten by the use of isotropic model are obtained. Tables 2 and 3 show clearly that the variation of the elastic modulus,  $E_{11}$ , has great effect on the stress components  $\sigma_r$  and  $\sigma_\theta$ . The radial stress  $\sigma_r$  increases significantly with the decreasing of  $E_{11}$ , and the zero point of  $\sigma_r$  on loading axis moves definitely. These are indeed the important factors which severely affect the accuracy of point-load tests<sup>[9]</sup>. Figs.5 and 6 show the distributions of the radial stress  $\sigma_r$  on the loading axis and

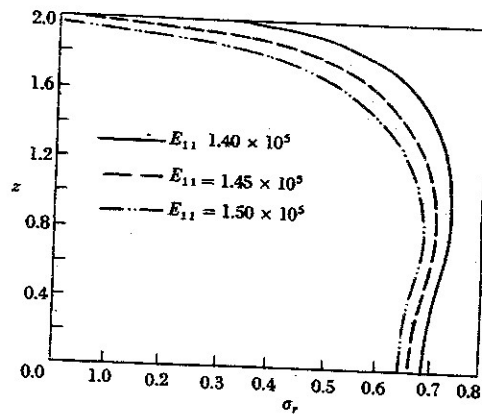
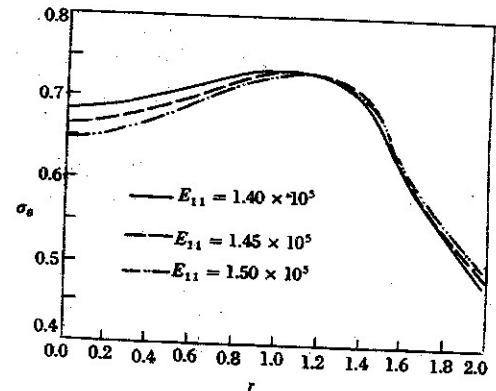


Fig.5 The radial stress on the loading axis

Fig.6 The circumferential stress on section  $z = 0$ 

the circumferential stress  $\sigma_\theta$  on the section  $z = 0$ , respectively. Finally, it should be pointed out that the larger is the ratio of  $E_{11}/E_\perp$ , the smaller the limiting break load of a specimen becomes. if the loading axis is chosen to be perpendicular to the isotropic plane of the material. Therefore, in order to get reliable data, the orientation of the isotropic plane of an irregular specimen<sup>[9]</sup> should be considered.

#### REFERENCE

- [1] Palamadov, V.P., *DAN*, 143, 6(1962), 1278 (in Russian).
- [2] Hu Haichang, *Acta Physica Sinica*, 10, 3(1954), 57(in Chinese).
- [3] Vendhan, C.P. and Archer, R.R., *Int. J. Solids Structures*, 14, 4(1978), 305.
- [4] Lekhniskii, S.G., *Theory of Elasticity of an Anisotropic Body*, Moscow, Mir. Pub., 1981
- [5] Eubanks, R.A. and Sternberg, E., *J.Rat. Mech. Anal.*, 3, 1(1954), 89.
- [6] Ding Haojiang, et al, *Acta Mechanica Solida Sinica*, 4(1983), 585(in Chinese).
- [7] Fama, M.E.D., *Quart. J. Mech. Appl. Math.*, 25, 4(1972), 479.
- [8] Yun Tianquan, et al, *Appl. Math. Mech.*, 2, 6(1981), 641(in Chinese).
- [9] The Research Group of Point-Load Tests, Dept. of Hydrogeology and Engineering Geology, College of Geology of Chendu, *Tests of Point-Load Rock Specimen*, Geology Press, 1979(in Chinese).